1/3-shot-noise suppression in diffusive nanowires

M. Henny, S. Oberholzer, C. Strunk, and C. Schönenberger
Institut für Physik, Universität Basel, Klingelbergstrasse 82, CH-4056 Basel, Switzerland
(Received 16 July 1998)

We report low-temperature shot-noise measurements of short diffusive Au wires attached to electron reservoirs of varying sizes. The measured noise suppression factor compared to the classical noise value $2e|I|$ strongly depends on the electric heat conductance of the reservoirs. For small reservoirs injection of hot electrons increases the measured noise, and hence the suppression factor. The universal 1/3 suppression factor can only asymptotically be reached for macroscopically large and thick electron reservoirs. A heating model based on the Wiedemann-Franz law is used to explain this effect. [S0163-1829(99)09203-6]

I. INTRODUCTION

Due to the quantization of the electrical charge in units of e, the electrical current fluctuates around its average value I. These fluctuations are known as shot noise.[1] At zero temperature, the spectral density S_I of shot noise is in general proportional to the average current and the charge quantum. At finite temperatures, thermal fluctuations give an additional contribution to the measured noise. In equilibrium, the spectral density of the thermal fluctuations (Johnson-Nyquist noise) is given by $S_I=4kT/R$ for a device with resistance R. From shot noise one can obtain information on the conduction mechanism not accessible from conventional resistance measurements, since it is directly related to the degree of randomness in carrier transfer caused by the electron scattering in the wire. If the number of transferred electrons in a given time interval is determined by a Poissonian distribution, the current shows shot noise with a value given by the well known Schottky formula[3] $S_{\mathrm{Poisson}}=S_I=2e|I|$. This classical shot noise is observed in tunnel junctions or vacuum tubes, for example.[4] Shot noise for wires connected to electron reservoirs on each end is lower than the classical shot-noise value S_{Poisson} by a factor that depends on the ratio of the wire length L with respect to characteristic scattering lengths like the elastic (l_e), electron-electron ($l_{e\text{-}e}$,), and electron-phonon ($l_{e\text{-}ph}$) scattering lengths. In a ballistic wire ($L \ll l_e$), shot noise vanishes, since scattering is completely absent.[5] In the diffusive regime ($L \gg l_e$), excess noise varies linearly with current only if $L \ll l_{e\text{-}ph}$. Two limiting cases can then be distinguished. In the interacting (electron) regime, i.e., $L \gg l_{e\text{-}e}$, the electrons assume a Fermi-Dirac distribution with a locally varying temperature above the phonon temperature. The noise is given by the Johnson-Nyquist noise of the mean electron temperature averaged over the whole wire length. Independent of material and geometric parameters, shot noise is reduced by a factor of $\sqrt{3}/4$ from the classical value.[6] On the other hand, in the noninteracting (electron) regime, i.e., $L \ll l_{e\text{-}e}$, the distribution function f is no longer a Fermi-Dirac function. For this regime various theories predict a fundamental shot-noise reduction factor of 1/3. Using the random-matrix theory, Beenakker and Büttiker have calculated this factor.[7] In their derivation, the conductor is implicitly assumed to be phase coherent and the factor is obtained as the ensemble-averaged value. In a semiclassical picture, where no phase-coherence is required, the fluctuations of the distribution function f yield surprisingly the very same suppression factor.[8] It was pointed out by Shimizu and Ueda that dephasing of the electrons indeed does not change the noise power in contrast to dissipation or nonideal reservoirs.[9] Moreover, the sequential transfer of electrons through a series of tunnel barriers has also been shown to lead to exactly the same noise reduction factor of 1/3 in the limit of a large number of barriers.[10] Recently, two publications have provided additional theoretical support for the universality of the magic 1/3 suppression factor. In the first, a nondegenerate diffusive conductor[11] is studied by computer simulations, while in the second, the universality is extended to multiterminal diffusive conductors with arbitrary shape and dimension.[12] Note that this reduction factor does not depend on any geometric parameter like length, width, or thickness, nor on the sample resistance.

The remarkable fact, that the same reduction factor of 1/3 is derived from different theoretical models, has been ascribed to a numerical coincidence by Landauer.[13] On the other hand, this identity may not be so astonishing, if one considers that the Drude conductance $G=G_0 N l_e/L$ can also be deduced quantum mechanically as well as classically. Both conductivity and noise rely on the same principles.[14]

Despite the remarkable universality of the reduction factor 1/3 obtained from various theoretical models for the noninteracting electron regime, a clear experimental confirmation in the asymptotic limit $eV \gg kT$, in which shot noise is much larger than thermal noise, is lacking. To clearly distinguish the noninteracting from the interacting regime by noise measurements, a relatively high accuracy is needed allowing us to separate the two close-lying reduction factors 1/3 and $\sqrt{3}/4$ from a measurement of noise, which by itself is a small quantity of order 10 $\mathrm{pV}/\sqrt{\mathrm{Hz}}$.

The first experiment in this field was done by Liefrink *et al.*[15] using a two-dimensional electron gas, which was electrostatically confined into a wire. A linear variation of the noise with current was found. The measured reduction factors, however, were ranging from 0.2 to 0.45. Steinbach *et al.*[6] found excellent agreement with the $\sqrt{3}/4$ theory for a Ag wire of 30 μm length, but reported a value between 1/3 and $\sqrt{3}/4$ for a 1-μm-long wire, although theory[16] predicts

 ©1999 The American Physical Society

$L \ll l_{e\text{-}e}$ for this length at 50 mK. Schoelkopf *et al.* were the first to study high-frequency (quantum-) shot noise of diffusive wires.[17] By comparing measured differential noise dS_I/dI with the 1/3 and $\sqrt{3}/4$ theories, good agreement was found for the noninteracting regime. However, the absolute slope, i.e., the 1/3 reduction factor, was not measured in the asymptotic limit $eV \gg kT$. An approach that allowed us to distinguish between the interacting and the noninteracting regimes, was introduced by Pothier *et al.*, who measured directly the distribution function $f(E,x)$ of a wire by tunneling spectroscopy.[18]

We will show in the present paper that the electron reservoirs connected to the wire are of great importance for the confirmation of the 1/3 suppression factor. Bounded by the limiting values 1/3 and $\sqrt{3}/4$, the measured noise-reduction factor can in principle distinguish between the noninteracting ($L \ll l_{e\text{-}e}$) and the interacting regime ($L \gg l_{e\text{-}e}$). This is, however, only true, if heating in the electron reservoirs is absent. As was remarked by Shimizu and Ueda, nonideal reservoirs can lead to additional noise when a current flows through the conductor.[9] Our experiments demonstrate that noise-reduction factors close to $\sqrt{3}/4$ can be measured, even though the wires are in the noninteracting regime. This is demonstrated to be caused by unavoidable reservoir heating, which results in a significantly increased measured slope of the shot noise in the asymptotic limit. We discuss noise measurements of three Au wires that mainly differ in the size of the attached electron reservoirs. The sample with the thickest reservoirs, i.e., the highest reservoir heat conductivity, closely approaches the universal 1/3-shot-noise reduction factor.

II. THEORY

A. Noise in diffusive conductors

The current flowing through a wire exhibits fluctuations $\Delta I = I(t) - I$ around the average current I. The spectral density of these current fluctuations, i.e., current noise, can be written as the Fourier transform of the current autocorrelation function:[19]

$$S_I(\omega) = 2\int_{-\infty}^{\infty} dt e^{i\omega t} \langle \Delta I(t+t_0)\Delta I(t_0)\rangle_{t_0}. \tag{1}$$

In thermodynamical equilibrium Eq. (1) yields $S_I = 4kT/R$, called thermal or Johnson-Nyquist noise.[2] Under current bias the individual charge pulses of the electrons give rise to out-of-equilibrium noise known as shot noise. If the electrons pass rarely and completely random in time governed by a Poissonian process, one obtains the classical shot noise $S_I = 2e|I|$ as derived by Schottky.[3] If in contrast the electron stream is denser, correlations due to many-particle statistics induced by the Pauli principle or due to Coulomb interaction can significantly reduce shot noise.[1] For $\hbar\omega \ll kT$ thermal and shot noise display a white spectrum (frequency independent). In contrast, resistance fluctuations related to the dynamics of impurities in the sample display in general so called $1/f$ noise proportional to $1/\omega$ over a large frequency range.[19] We restrict ourselves to a frequency range, which is high enough to safely neglect the $1/f$ noise.

An elegant framework to describe the shot-noise power of a mesoscopic device is the Landauer-Büttiker formalism.[20] It is valid in linear response and in the absence of inelastic scattering. The current is carried by independent parallel channels with a transmission probability T_n. The conductance is then written as $G = (e^2/h)\Sigma_n T_n$ and the shot noise at zero temperature reads[21]

$$S_I = 2e|V|\frac{e^2}{h}\sum_n T_n(1-T_n). \tag{2}$$

A diffusive wire is described as an ensemble of many parallel channels. Random-matrix theory predicts a bimodal distribution function for transmission probabilities, which leads to a suppression of shot noise by a factor of 1/3 compared to its classical value:[7]

$$S_I = \frac{1}{3}2e|I|. \tag{3}$$

Nagaev proposed a semiclassical approach to determine the noise in a diffusive wire.[8] Starting from a kinetic equation for the electron occupation probability $f(E,x)$, current noise is shown to be related to the fluctuations of the occupation number given by $f(1-f)$. Explicitly, the following equation was derived:

$$S_I = 4G\left\langle \int_{-\infty}^{\infty} f(E,x)[1-f(E,x)]dE \right\rangle_{wire}. \tag{4}$$

In this approach, phase coherence is not required in contrast to the random-matrix theory. Furthermore, it has the advantage that inelastic scattering processes can easily be included. They are introduced by scattering integrals I_{ee} for electron-electron scattering and I_{ph} for electron-phonon scattering. f can be obtained by the following diffusion equation:

$$D\frac{d^2}{dx^2}f(E,x) + I_{ee}(E,x) + I_{ph}(E,x) = 0, \tag{5}$$

where D is the diffusion coefficient of the electrons.[22] The boundary conditions are given by Fermi-Dirac distributions with $f(E,0) = [\exp(E/kT)+1]^{-1}$ for the left reservoir and $f(E,L) = \{\exp[(E-eV)/kT]+1\}^{-1}$ for the right reservoir. It is assumed that the reservoirs keep the two ends of the wire at constant electrochemical potential 0 and eV, respectively, and at a constant temperature T (Fig. 1 bottom left). If inelastic scattering is absent (noninteracting regime), the solution of Eq. (5) is a linear combination of the two reservoir distribution functions ($0 \leqslant x \leqslant L$):

$$f(E,x) = \frac{L-x}{L}f(E,0) + \frac{x}{L}f(E,L), \tag{6}$$

which has the shape of a two-step function (Fig. 1 bottom right). Inserting this into Eq. (4) one obtains for the noise

$$S_I = \frac{2}{3}\left[\frac{4kT}{R} + \frac{eV}{R}\coth\left(\frac{eV}{2kT}\right)\right]. \tag{7}$$

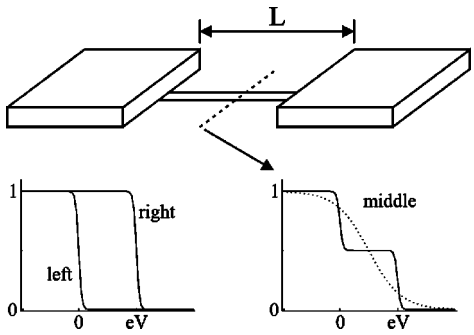

FIG. 1. The electron-distribution function of a wire connected to two large reservoirs at its ends is shown for the case of an applied voltage V. In the reservoirs and at the wire ends the distribution function is a Fermi-Dirac distribution at the chemical potential 0 and eV (bottom left). Within the wire it is a two-step function if no inelastic scattering is present, $L \ll l_{e\text{-}e}$ (solid line) or it is a Fermi-Dirac distribution with an effective electron temperature kT_e being of the order eV if $L \gg l_{e\text{-}e}$ (dashed line).

This equation is identical to the result obtained with the Landauer-Büttiker formalism and describes the crossover from thermal noise at $V=0$ to an asymptotic shot-noise behavior $S_I = \frac{1}{3} \times 2e|I|$ for $eV \gg kT$. As mentioned above, the same reduction factor also results from a model using sequential tunneling through a series of tunnel barriers. Although various theories predict a universal 1/3 noise-reduction factor for the noninteracting regime, no experiment has yet confirmed the 1/3 slope in the asymptotic limit $eV \gg kT$.

Another special case arises if $L \gg l_{e\text{-}e}$. The electrons can exchange energy among each other and are, therefore, in a local thermodynamic equilibrium. Hence, the occupation probability $f(E,x)$ is described by a Fermi-Dirac distribution with a *local* electron temperature $T_e(x)$ at the electrochemical potential $\mu(x) = (x/L)eV$:

$$f(E,x) = \frac{1}{e^{[E-\mu(x)]/kT_e(x)}+1}. \tag{8}$$

The temperature profile $T_e(x)$ along the wire can again be calculated from Eq. (5), which reduces to a heat-flow equation:

$$\frac{\mathfrak{L}_0}{2}\frac{d^2T_e^2}{dx^2} = -\left(\frac{V}{L}\right)^2 + \Gamma\left(\frac{k}{e}\right)^2 (T_e^5 - T^5), \tag{9}$$

where $\mathfrak{L}_0 = (\pi^2/3)(k/e)^2$ is the Lorenz number and Γ is a parameter describing electron-phonon scattering. Equation (4) turns now into $S_I = 4k\langle T_e\rangle_x/R$. Hence, the excess noise is now solely due to thermal noise of the hot electrons and S_I is determined by the electron temperature averaged over the whole wire length. For $L \ll l_{e\text{-}ph}$ the electron-phonon term can be neglected and an analytical solution exists for the temperature profile (inset Fig. 2):[23]

$$T_e(x) = \sqrt{T^2 + \frac{x}{L}\left(1 - \frac{x}{L}\right)\frac{V^2}{\mathfrak{L}_0}}. \tag{10}$$

This leads to

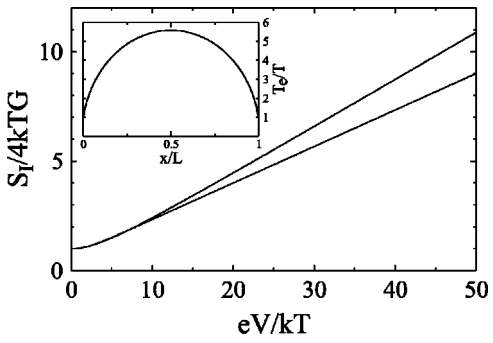

FIG. 2. Calculated noise power for the noninteracting regime $L \ll l_{e\text{-}e}$ (lower curve) and for the interacting regime where $L \gg l_{e\text{-}e}$ (upper curve). To distinguish between the two regimes in the asymptotic limit a ratio of at least $eV/kT \simeq 10$ is required. The inset shows the temperature profile in the interacting regime along the wire for $eV/kT = 20$.

$$S_I = \frac{2kT}{R}\left[1 + \left(\nu + \frac{1}{\nu}\right)\arctan\nu\right], \tag{11}$$

with $\nu = \sqrt{3}eV/2\pi kT$. For $eV \gg kT$ one obtains $S_I = \sqrt{3}/4 \times 2e|I| \simeq 0.43 \times 2e|I|$.

Figure 2 displays the expected noise vs applied voltage for the noninteracting regime according to Eq. (7) and for the interacting electron picture according to Eq. (11). Both curves start at $V=0$ with thermal noise and separate into two straight lines with different slopes for $eV \gg kT$. The figure suggests that at least $eV/kT \gtrsim 10$ is necessary in order to distinguish the two regimes by the measured asymptotic slopes. An experiment under such highly nonequilibrium conditions requires special care in the treatment of dissipation due to the large unavoidable power input. In particular, one has to consider how energy is removed in the reservoirs attached to the wire.

B. Reservoir heating

The theory described above assumes ideal boundary conditions for the electrons at the immediate wire end. The electrons in the reservoirs are described by a Fermi-Dirac distribution with a constant electrochemical potential μ and a constant bath temperature T independent of the current flowing through the wire. This assumption is only correct for reservoirs of infinite size with infinite electric and heat conductivities. For real reservoir materials, e.g., Au, Ag, and Cu, the actual size and heat conductance of the reservoirs will matter. In the following sections we discuss the different contributions that can give rise to a temperature increase in the reservoirs caused by the generated power V^2/R, which has to dissipate in the reservoir and substrate. It will turn out that noise is substantially affected in the noninteracting regime, if the reservoir temperature rises. The heat flows through a chain of different thermal resistors connected in series (see Fig. 3). We start at the top of the heat chain where the electronic heat spreads out radially into the whole reservoirs. We take the radius of the two inner semicircles to be $r_1 = l_{e\text{-}e}/2$. For the noninteracting regime these semicircles may be considered as part of the wire itself (the inner white part in Fig. 3). This is justified since the 1/3 suppression has been shown to hold independent of the wire geometry, as

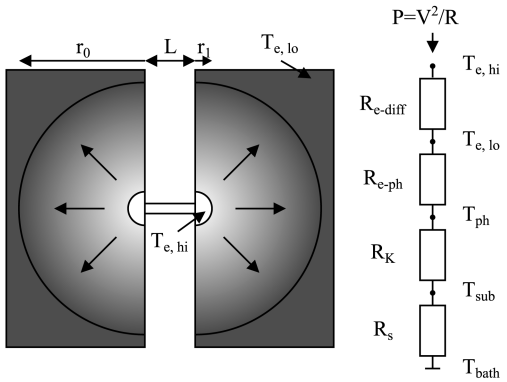

FIG. 3. The power V^2/R produced in the wire has to be dissipated in the reservoirs and in the substrate. For that it has to pass a series of thermal resistors. First, it is distributed in the reservoir by diffusion. Then, the heat is transferred by electron-phonon scattering into the phonon system of the reservoir from where it flows into the substrate and finally into the cryogenic bath kept at the constant temperature T_{bath}. Over every thermal resistor a temperature drop proportional to the resistance and power is induced.

long as the wire is shorter than $l_{e\text{-}e}$.[12] Since a change in temperature is only defined over distances larger than $l_{e\text{-}e}$, we assume a constant temperature in this inner region. This is the highest temperature and denoted with $T_{e,hi}$. Going radially outwards, the power spreads by electronic heat diffusion in the electron gas, which is described by a thermal spreading resistance $R_{e\text{-}diff}$, similar to the well known electrical spreading resistances. The transfer of energy from the electron gas to phonons in the reservoirs can be neglected up to a radius of order $l_{e\text{-}ph}$. For higher radii the electron-phonon scattering length provides a natural cutoff for the electronic heat diffusion. We, therefore, define the largest radius r_0 to be the smaller of either $l_{e\text{-}ph}$ or the planar reservoir size L_{res}. At this distance the electron temperature has dropped to $T_{e,lo}$. In the heat-chain model, the thermal resistance for the conversion of energy from electronic to lattice degrees of freedom follows next. First, energy flows into the phonon system of the reservoir resulting in a difference between $T_{e,lo}$ and the reservoir phonon temperature T_{ph}. The corresponding thermal resistance is denoted by $R_{e\text{-}ph}$. Then, a thermal-boundary resistance R_K (Kapitza resistance) may give rise to a difference in phonon temperatures of reservoir T_{ph} and substrate T_{sub}. Finally, the generated heat is transferred into the cryogenic bath, held at the constant bath temperature T_{bath}. This thermal anchor to the bath has the thermal resistance R_s. The temperature difference over each thermal resistor is proportional to the thermal resistance and the power P flowing through it. The minimization of all thermal resistances in the complete heat chain is essential to prevent $T_{e,hi}$ to rise and thus to prevent the injection of hot electrons into the wire. This is particularly important for the noninteracting regime, since it turns out that a temperature rise in this regime results in substantial additional noise in the asymptotic limit. This can be understood from the asymptotic behavior of Eq. (7) for $eV \gg kT$, which contains a temperature-dependent offset in addition to the term linear in I:

$$S_I = \frac{1}{3} 2e|I| + \frac{8}{3} kT/R. \tag{12}$$

For the temperature T, we have to insert $T_{e,hi}$ into Eq. (12) as the temperature of the injected electrons. If $T_{e,hi}$ scales linearly with the current I, the measured slope will be larger than 1/3. It is quite remarkable that in the interacting regime an increase of $T_{e,hi}$ has only a minor effect for the measured noise. As the linear asymptote for $eV \gg kT$ passes through the origin, the correction to the slope is only of second order in kT/eV.

Next we estimate the increase of the four temperatures in the heat chain $T_{sub}, T_{ph}, T_{e,lo}$, and $T_{e,hi}$, when a heat current flows through the chain. The connection between sample and cryogenic bath determines the increase of T_{sub}. We will see later in the experimental section that its dependence on the power P is phenomenologically best described as

$$T_{sub} = (T_{bath}^2 + aP)^{1/2}, \tag{13}$$

where a describes the thermal coupling of the sample to the cryogenic bath.

A possible difference between T_{ph} and T_{sub} is due to a Kapitza resistance and can be written as[24]

$$T_{ph} = \left(T_{sub}^4 + \frac{P}{A\sigma_K} \right)^{1/4}. \tag{14}$$

A denotes the area of the reservoir and σ_K is a parameter specific for the interface between reservoir and substrate. Because of the large size of the reservoirs in this work, this is a small effect, but was added here for completeness.

To calculate the difference between electron temperature $T_{e,lo}$ and phonon temperature T_{ph} in the reservoir, we assume for simplicity that the electron temperature is constant over the whole reservoir. When we multiply Eq. (9) with the electrical conductivity σ, the second term on the right-hand side $\sigma(k/e)^2\Gamma(T_{e,lo}^5 - T_{ph}^5)$ is the power per volume dissipated by electron-phonon scattering and can be set equal to V^2/RAt. σ is now the electrical conductivity of the reservoir and t its thickness. We obtain

$$T_{e,lo} = \left[T_{ph}^5 + \frac{V^2}{R} \frac{R_\square}{\Gamma A} \left(\frac{e}{k} \right)^2 \right]^{1/5}, \tag{15}$$

where we have introduced the sheet resistance of the reservoir $R_\square = 1/(\sigma t)$. The parameter Γ is known from noise measurements on long diffusive wires ($L \gg l_{e\text{-}ph}$),[24–26] and can be used to determine the electron-phonon scattering length[24] $l_{e\text{-}ph} = 1.31/\sqrt{T^3\Gamma}$.

Finally, in order to determine the temperature in the wire $T_{e,hi}$, we have to calculate the temperature gradient in the reservoir due to radial electronic heat diffusion from the inner semicircles with radius r_1 to the outer ones with radius r_0 (see Fig. 3). Using cylindrical symmetry the heat-flow density is given by

$$\vec{j} = -\kappa \vec{\nabla} T = \frac{P}{2\pi r t} \vec{e}_r, \tag{16a}$$

where r is the radius of a semicircle between r_1 and r_0, t the thickness of the reservoir, and κ the electronic thermal conductivity derived from the Wiedemann-Franz law $\kappa = \mathfrak{L}_0 T\sigma$, the latter has been shown to be valid in small

wires.[6,26] Integrating over the temperature gradient $\vec{\nabla}T$ with the boundary condition $T(r_0)=T_{e,lo}$, yields for $T_{e,hi}=T(r_1)$:

$$T_{e,hi}^2=T_{e,lo}^2+b^2V^2, \tag{16b}$$

with

$$b=\sqrt{\frac{1}{\pi \pounds_0}\frac{R_\square}{R}\ln\frac{r_0}{r_1}}. \tag{16c}$$

For large applied voltages, the second term on the right-hand side of Eq. (16b) dominates and a linear dependence of the electron temperature with respect to the applied voltage is obtained:

$$T_{e,hi}=bV. \tag{16d}$$

When inserting Eq. (16d) into Eq. (12), the increase in noise ΔS_I can be calculated and one obtains for the additional slope

$$\frac{\Delta S_I}{2eI}=\frac{4}{3}\frac{k}{e}b=\frac{4}{3}\sqrt{\frac{3}{\pi^3}\frac{R_\square}{R}\ln\frac{r_0}{r_1}}. \tag{16e}$$

Hence, even in the independent-electron regime the measured slope is always larger than 1/3. The increase in slope is determined by the ratio $R_\square/R$ and the geometrical parameters r_0 and r_1. The electrical parameters $R_\square$ and R are known accurately. For the radii natural cutoffs have been introduced: $l_{e\text{-}e}/2$ for r_1 and the smaller of either $l_{e\text{-}ph}$ or the reservoir size L_{res} for r_0. Though the assumed values for r_0 and r_1 are correct on physical grounds, a more rigorous theory may give a slightly different prefactor. Since r_0 and r_1 enter Eq. (16e) only logarithmically, corrections are small. Both $l_{e\text{-}e}(T)$ and $l_{e\text{-}ph}(T)$ display a power-law dependence on temperature T effectively resulting in the cutoff term $\ln(r_0/r_1)$ to be temperature dependent as well, albeit weakly, only proportional to $\ln(T)$. This weaker temperature dependence will be neglected in the following. For r_0 and r_1, values typical for the experiment will be used.

In the following we compare the magnitude of the temperature increase caused by electronic heat diffusion using Eq. (16b) and electron-phonon scattering using Eq. (15). In Fig. 4 the relative increase $\Delta T/T$ is plotted as a function of bath temperature T for fixed $eV/kT=20$, which is a typical value used to distinguish between the interacting and noninteracting regime. Within the above-mentioned assumption, the contribution from electronic heat diffusion is independent of T, the two plotted values (dashed lines) correspond to a ratio of $R/R_\square=250$ and $R/R_\square=1000$ with $r_0/r_1=100$. In contrast, the electron-phonon coupling strongly depends on T. Its thermal resistance increases with decreasing temperature, since the electron-phonon scattering rate is proportional to T^3. This results in a drastic increase of $\Delta T/T$ at low temperatures in Fig. 4 (solid curves correspond to different lateral reservoir sizes as denoted). Due to this sharp rise the study of nonequilibrium effects at very low temperatures becomes increasingly difficult.[25] The large-temperature increase due to the vanishing coupling of the electrons to phonons at low temperatures can only be compensated by enlarging the reservoir volume. Note that both contributions depend on the reservoir thickness, which is included in the reservoir sheet resistance $R_\square$.

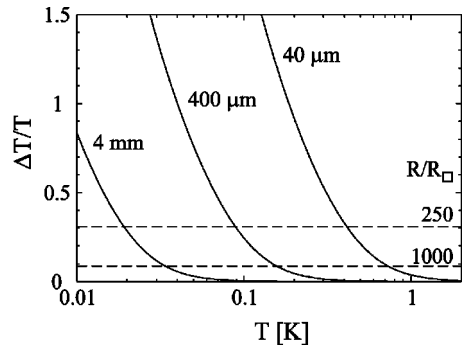

FIG. 4. The relative temperature difference $\Delta T/T$ is plotted for $eV/kT=20$ as a function of T for various types of reservoirs. The relative increase due to $R_{e\text{-}diff}$ (dashed lines) strongly depends on the ratio wire resistance R to reservoir sheet resistance $R_\square$. The contribution from electron-phonon scattering (solid lines) is strongly temperature dependent and increases with decreasing temperature. Its magnitude depends mainly on the reservoir's lateral size (denoted next to the curve), the electron-phonon scattering parameter (here $\Gamma=5\times10^9\ \mathrm{K}^{-3}\,\mathrm{m}^{-2}$), and the ratio $R/R_\square$ (here 250).

Up to now, as a first approximation, we have treated electronic heat diffusion and electron-phonon scattering independently. This is certainly not fully correct. The electron temperature, which is relevant for the electron-phonon scattering, is not constant over the reservoir as previously assumed. To determine the temperature profile self-consistently, we can combine the electronic heat diffusion and the electron-phonon scattering term in one equation, which has a similar form as Eq. (9), but now in cylindrical coordinates. We assume that the voltage drop across the reservoirs is negligible, so that the heat-generating term can be omitted:

$$\frac{\pounds_0}{2}\left[\frac{d^2T_e^2}{dr^2}+\frac{T_e}{r}\frac{dT_e}{dr}\right]=\Gamma\left(\frac{k}{e}\right)^2(T_e^5-T_{ph}^5). \tag{17a}$$

The power enters the system at a semicircle of radius r_1 defining the first boundary condition. According to Eq. (16a) it is given by

$$\frac{\pounds_0}{2}\frac{d}{dr}T^2(r_1)=\frac{P}{2\pi r_1}R_\square. \tag{17b}$$

We now assume the reservoir to be terminated by a semicircle of radius r_0. The heat flow at the end of the reservoir must vanish and the second boundary condition reads

$$\frac{\pounds_0}{2}\frac{d}{dr}T^2(r_0)=0. \tag{17c}$$

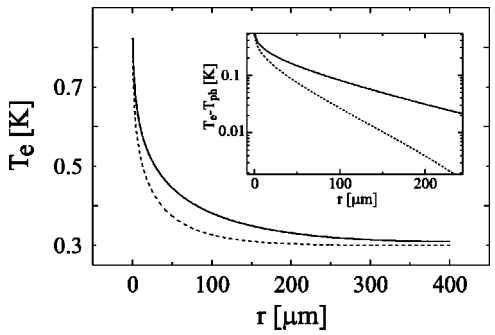

FIG. 5. Resulting temperature profile in the reservoir obtained from a computer simulation using the method of finite elements. For an incoming power of 200 nW and a reservoir sheet resistance $R_{\square}=42\ \mathrm{m}\Omega$, the electron temperature $T_{e,hi}$ rises from 0.3 to 0.8 K. The curves are calculated with different electron-phonon scattering parameters: $\Gamma=5\times10^{9}\ \mathrm{K}^{-3}\,\mathrm{m}^{-2}$ for the dashed line ($l_{e\text{-}ph}=110\ \mu\mathrm{m}$) and $\Gamma=1\times10^{9}\ \mathrm{K}^{-3}\,\mathrm{m}^{-2}$ for the solid line ($l_{e\text{-}ph}=250\ \mu\mathrm{m}$). The inset shows the logarithmic behavior of the same graphs but after subtracting the phonon temperature of 0.3 K from the electron temperature.

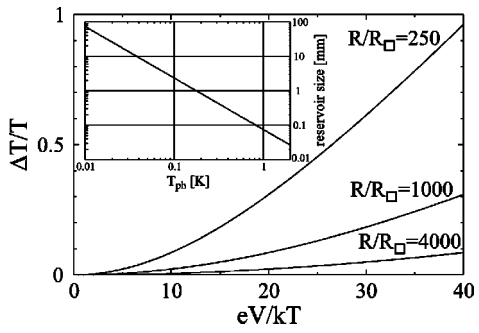

FIG. 6. Calculated temperature increase $\Delta T/T$ due to electronic heat diffusion as a function of applied voltage. A linear variation follows if $eV/kT\gg\sqrt{R/R_{\square}}$. The inset shows the lateral reservoir size necessary to prevent a temperature increase due to electron-phonon scattering. It is given by $4l_{e\text{-}ph}=5.24/\sqrt{T^{3}\Gamma}$ with $\Gamma=5\times10^{9}\ \mathrm{K}^{-3}\,\mathrm{m}^{-2}$.

The differential equation (17a) together with the boundary conditions (17b) and (17c) cannot be solved analytically. To obtain quantitative estimates for $T_{e,hi}$, we have performed a simulation using the method of finite elements. We have varied the power P, the electron-phonon scattering parameter Γ, and the reservoir outer and inner radii r_0 and r_1. The main results are as follows: The electron-temperature decays approximately exponentially from $T_{e,hi}$ at the inner radius r_1 to a base temperature $T_{e,lo}$ at r_0. The decay length, over which T_e-T_{ph} is reduced by a factor e, is about $l_{e\text{-}ph}/4$, where $l_{e\text{-}ph}$ is the electron-phonon scattering length at $T_{e,lo}\simeq T_{ph}$. The resulting temperature profile of two simulations with different Γ is plotted in Fig. 5. The inset shows the difference T_e-T_{ph} on a logarithmic scale. The two straight slopes indicate the exponential decay of the temperature T_e to T_{ph}. The decay length depends only slightly on the power P. If $r_0\gtrsim 2l_{e\text{-}ph}$ no significant raise of $T_{e,lo}$ with respect to T_{ph} is found and $T_{e,hi}$ depends only on the incoming power and the reservoir sheet resistance. This corresponds to the limit described above, where the electron-phonon contribution is small compared to the one from electronic heat diffusion. It can be used as a design criterion for reservoirs appropriate in minimizing dissipative reservoir heating. The reservoir size, which is required for this, is plotted as a function of T_{ph} in the inset of Fig. 6. The simulation also shows that the functional behavior of $T_{e,hi}$ with applied voltage V can be described as in Eq. (16b). The relation $b\propto\sqrt{R_{\square}/R}$ is still valid consistent with Eq. (16c) and the proportionality factor corresponds to a ratio of about $r_0/r_1=100$, which is very reasonable. Such a ratio would also follow from our simple analytical model, when the electron-phonon scattering length is inserted for r_0 and the electron-electron scattering length for r_1 taken at subkelvin temperatures. This discussion shows that large reservoirs are needed to minimize the increase in reservoir temperature. In particular, if $L_{res}\gg l_{e\text{-}ph}$ is followed in the design of the reservoirs, the main contribution for the relative temperature rise $\Delta T/T$ is caused by electronic heat diffusion, which is displayed in Fig. 6 as a function of the applied voltage for three different ratios of $R/R_{\square}$. As can be seen, the temperature increase can be substantial.

III. EXPERIMENT

A. Design

In the experiments described below we explore the 1/3-shot-noise suppression in the noninteracting regime and study the influence of different reservoir configurations. In view of the important role of the reservoirs discussed above, a careful design of the experiment is crucial. The noninteracting regime requires $L\ll l_{e\text{-}e}$. For an estimate of $l_{e\text{-}e}$ we use Altshuler's formula valid for a one-dimensional wire:

$$l_{e\text{-}e}=\left[\left(\frac{\sqrt{2}}{k_B}\right)\left(\frac{\hbar}{e}\right)^{2}\frac{Dw}{TR_{\square}^{w}}\right]^{1/3}, \tag{18}$$

where w is the width and $R_{\square}^{w}$ the sheet resistance of the wire.[16] For a typical Au wire with a thickness of 15 nm, diffusion coefficient $D=120\ \mathrm{cm}^2/\mathrm{s}$, width $w=100$ nm, and $R_{\square}^{w}=2.3\ \Omega$, we find a scattering length $l_{e\text{-}e}=4.2\ \mu$m at 0.3 K. Using standard e-beam lithography, a wire with a length of 1 μm connected to two reservoirs is feasible. Shorter wires are difficult to fabricate because of the proximity effect from exposing the large areas of the two reservoirs.

As mentioned above, in order to distinguish the 1/3 from the $\sqrt{3}/4$ regimes a ratio of at least $eV/kT\gtrsim 10$ is necessary. A low-base temperature is required, since otherwise the applied voltage becomes too high and electron-phonon scattering in the wire is unavoidable. To get an estimate of the influence of electron-phonon scattering on noise we have to compare the wire length with the electron-phonon scattering length at temperature eV/k. We find that a deviation in noise of about 1% would result if $L\simeq 4l_{e\text{-}ph}$. For a 1-μm-long wire with $\Gamma=5\times10^{9}\ \mathrm{m}^{-2}\ \mathrm{K}^{-3}$ this relates to a maximum voltage, which corresponds to 17.6 K. For a ratio of $eV/kT=40$ (the largest ratio used in the experiment), the bath temperature shall be lower than 440 mK. As explained above the reservoir heating strongly depends on the ratio $R_{\square}/R$, which ought to be as small as possible to avoid heating. In our experiment we will vary this ratio. As we have fixed the length of the wire, its width and thickness should be small to

TABLE I. Sample parameters at 0.3 K.

	R_{tot} (Ω)	#	$\overline{R}$ (Ω)	L (nm)	w (nm)	Reservoir	$R_\square$ (mΩ)	$(R_\square/\overline{R})^{1/2}$
AI	329	28	11.8	910	160	200-nm Au	42	0.060
B	129	6	21.5	940	100	200-nm Au	42	0.044
AII	74.6	8	9.3	910	170	200-nm Au+1-μm Cu	2.8	0.018

achieve a high wire resistance. On the other hand, the reservoirs have to be as thick as possible and made of a highly conductive metal to reduce $R_\square$.

The size of the reservoirs has to be chosen according to the electron-phonon scattering length $l_{e\text{-}ph}$ in the reservoir. Its radius r should be about twice $l_{e\text{-}ph}$ to avoid a significant difference between electron and phonon temperature (see inset of Fig. 6). With $\Gamma=5\times10^9$ $\mathrm{m}^{-2}\,\mathrm{K}^{-3}$ we obtain $l_{e\text{-}ph}=1.31/\sqrt{T_e^3\Gamma}=110$ μm at 0.3 K, which means that two rectangles with 200 μm$\times$ 400 μm on each side are sufficient.[26] Note, that for 50 mK this length even exceeds 1.5 mm.

An estimate also has to be made for the temperature increase due to a Kapitza resistance. As a worst case estimate for σ_K we use 100 $\mathrm{W/m^2\ K^4}$. With a heating power of 50 nW we expect a temperature increase of only 25 mK, which is small compared to the applied voltage $eV/k=12$ K.

In our experiment, a possible increase of the substrate temperature T_{sub} is taken into account, since we can measure T_{sub} directly with noise thermometry using an additional monitor wire on the same substrate.

B. Sample fabrication

The samples were produced with standard *e*-beam lithography. A 600-nm-thick PMMA resist was spun on an oxidized Si(100) wafer and structured with a JEOL JSM-IC 848 at an acceleration voltage of 35 kV. The pattern consisted of a line (line dose ~1.8 nC/cm) and of two areas on each side of the line. To correct for the proximity effect the area dose was increased in steps from the wire ends (~200 $\mu\mathrm{C/cm^2}$) to the outer part of the reservoirs (400 $\mu\mathrm{C/cm^2}$). The small structures were written with a probe current of 40 pA and the large pads with 16 nA. In order to enable a second lithography step eight alignment marks were written. This structure was repeated up to 40 times on the same substrate. The resist was developed in $MiBK{:}IPA=1{:}3$ during 45 s. Metal evaporation was performed with the two-angle evaporation technique.[26] First a 15-nm Au layer was evaporated under normal incidence. Then for the reservoirs a second 200-nm Au layer was evaporated at a tilt angle of 30° without breaking the vacuum. This ensures a good contact between the wire and the reservoir. Even larger reservoirs were produced in a second lithographic step in which 1-μm-thick Cu layers were aligned over the previous reservoirs. Relevant parameters of the three samples are summarized in Table I.

C. Noise measurement setup

The lower inset of Fig. 7 shows the noise measurement setup. The sample with resistance R is biased by a current provided by the constant voltage source connected to large series resistors $R_s \gg R$. The voltage over the sample is then amplified with a gain of 1000 by two independent low-noise preamplifiers (EG&G 5184) operated at room temperature. The noise spectrum is obtained by a cross correlation of the two amplifier signals using a spectrum analyzer (HP 89410A). This correlation scheme effectively reduces voltage-offset noise from the preamplifiers.[27] For every data point the signal is averaged over a frequency bandwidth of 70 kHz at a typical center frequency of 300 kHz (at this frequency $1/f$ noise is absent). With a measuring time of 60 s a sensitivity of 10^{-22} $\mathrm{V^2\,s}$ is achieved. As we measure the voltage fluctuations $S_V=S_I R^2$, the signal $S_V=\frac{1}{3}\times2eVR$ is proportional to R. We aimed at a precision of 1% at a ratio $eV/kT=40$, which gives us a lower limit for the sample resistance of $R=90$ Ω. Within the geometrical requirements the typical resistance is, however, in the range of $10-20$ Ω. To increase the sample resistance and with it the precision, we use a series of many identical wires, all attached to individual reservoirs. The resistance of each wire was first measured at room temperature to obtain the scattering ΔR around the average resistance $\overline{R}$.

For an absolute noise measurement, a calibration of the complete setup is unavoidable. The measured noise signal is affected by shunt capacitances from the leads in the cryostat, which partially diminish the dynamical signal. We calibrate the measured excess noise against the thermal noise of the same sample measured within the same frequency bandwidth. This is done for every sample separately, since the resistance varies from sample to sample. A typical calibration is shown in Fig. 7. The thermal noise of the sample varies linearly with temperature T according to $S_U=4kTR$ with an offset, which arises from current noise of the preamplifiers. Since the resistance R is known from an independent

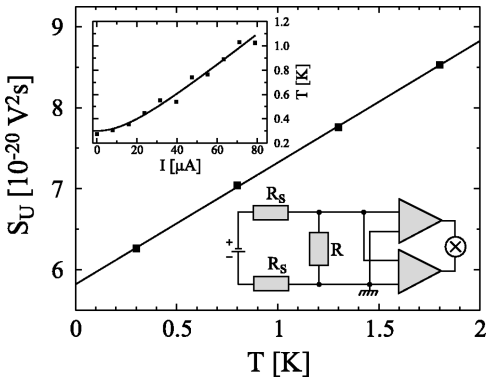

FIG. 7. Thermal noise of sample AI used for the calibration of the noise measurement setup sketched in the lower inset. The upper inset shows the substrate temperature measured on an additional unbiased monitor wire as a current flows through the sample.

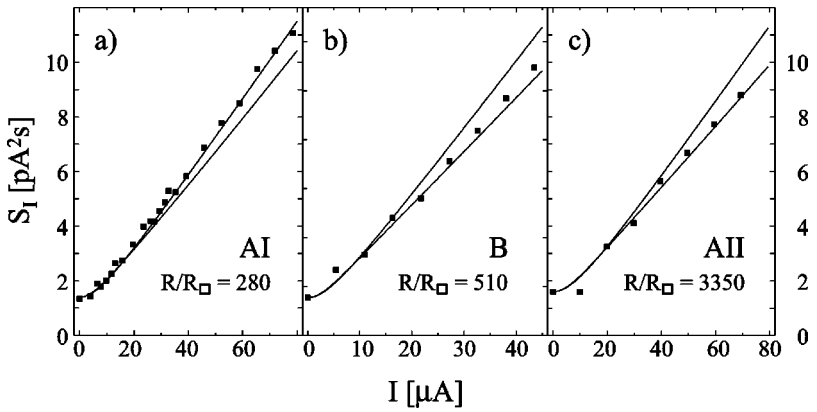

FIG. 8. Shot-noise measurements for three different samples with different ratio $R/R_{\square}$ at a bath temperature $T_{bath}=0.3$ K. The upper line corresponds to the prediction of $L \gg l_{e\text{-}e}$ (asymptotic slope $\sqrt{3}/4$), the lower one to $L \ll l_{e\text{-}e}$ (slope 1/3). The measured noise is significantly increased due to reservoir heating depending on $R/R_{\square}$.

dc measurement, the slope and offset of the line in Fig. 7 provides us with the absolute calibration.

As mentioned above, the substrate heating is determined from the thermal noise of an unbiased monitor wire on the same substrate. A typical measurement is displayed in the upper inset of Fig. 7. The dependence of the data could best be accounted for by the phenomenological relation $T_{sub}=(T^2+aP)^{1/2}$. It yields as fit parameter $a=1.31\times10^5\,\mathrm{K^2/W}$, which is specific for the cryostat.

IV. RESULTS AND DISCUSSION

We now discuss the experimental results for three different samples, which mainly differ in the heat conductance of their reservoirs. In Fig. 8 the measured shot noise of the samples (AI, B, AII) is plotted. The solid lines are calculated assuming noninteracting electrons (lower curve, slope 1/3) and interacting electrons (upper curve, slope $\sqrt{3}/4$). Two corrections are included in these theoretical lines: the increased substrate temperature using the parameter a and the relative scattering of the wire resistances around its average $\Delta R/\overline{R}$, which has, however, only a small influence of around 1%. The relevant sample parameters are summarized in Table I.

Sample AI consists of 28 wires with an average resistance of $\overline{R}=11.8\ \Omega$ and 200-nm-thick Au reservoirs resulting in a reservoir sheet resistance of $R_{\square}=42\ \mathrm{m\Omega}$. In Fig. 8(a) the measured noise of this sample as a function of current is shown. Within the accuracy of the experiment, the data points lie on the $\sqrt{3}/4$ curve and one may on first sight infer that the length of the wire (910 nm) is much longer than the electron-electron scattering length in contradiction to Eq. (18). This conclusion is, however, only valid if reservoir heating is completely absent.

For sample B the same wire length and reservoir thickness are used. Since the wires of this sample are narrower, their resistances R are higher, so that we expect to have less heating as compared to sample AI, since $R_{\square}/\overline{R}$ is reduced. As is evident from Fig. 8(b) the measured noise is indeed much lower, lying closer to the 1/3 curve than to the $\sqrt{3}/4$ curve. For the highest applied voltage we have $eV/kT\simeq35$ in both cases.

In order to increase $R/R_{\square}$ even further, we have fabricated thicker reservoirs with a much lower sheet resistance. Sample AII has initially been the same as sample AI, but in a second lithography step a 1-μm-thick Cu layer has been evaporated onto the reservoirs in addition to a thin Au layer preventing oxidation of the Cu reservoir (see Fig. 9). This reduces the reservoir sheet resistance considerably to 2.8 mΩ. During the second processing of the sample, several wires were lost and only eight of them remained for the measurement of sample AII. Because of the reduced total resistance R_{tot}, the measured noise voltage is lower, thus increasing the scatter in the data points, but a clear reduction of the slope is visible when comparing with the measurement of sample AI [see Figs. 8(a) and 8(c), respectively]. The data points are now consistent with the 1/3 prediction.

Since an asymptotic slope of 1/3 is the prediction for the noninteracting electron regime, sample AII has to be in this regime and, therefore, also AI (same wires), even though the latter displays a significantly increased noise indistinguishable from an asymptotic $\sqrt{3}/4$ slope. Since the wires used for sample B are made from the same material with a similar length, sample B must be in the independent regime as well. All three samples are in the noninteracting regime according to the theoretical estimate given above. However, only for sample AII with the highest conducting reservoirs does the measured noise correspond to the prediction for this regime.

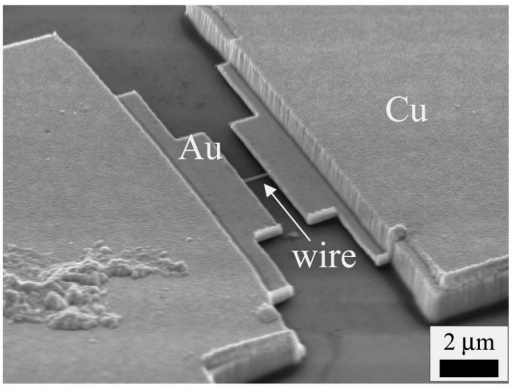

FIG. 9. Scanning electron microscopy micrograph of sample AII. The Au wire is terminated by 200-nm-thick Au reservoirs. In an overlaid second lithography step an additional layer of 1-μm Cu is evaporated to increase the reservoir thermal conductance.

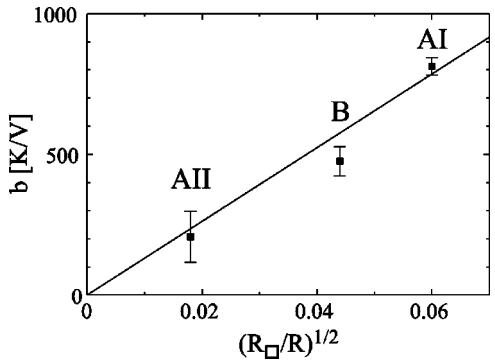

FIG. 10. The parameter b, which describes the enhancement of the measured noise by heating, is extracted from the data of Fig. 8. It is proportional to $\sqrt{R_\square/R}$. The origin of the graph corresponds to a slope of 1/3 expected for ideal reservoirs $R_\square=0$.

For the other two samples additional noise is detected, which increases as $R/R_\square$ becomes smaller.

We explain this increase of noise with electron heat diffusion in the reservoirs. Since we have estimated $R_{e\text{-}diff}$ to be the dominant thermal resistance for all reservoirs in this work, we expect from our model, that the temperature of the electrons injected into the wires to vary as $T_{e,hi}=(T_{sub}^2+b^2V^2)^{1/2}$ according to Eq. (16b). Inserting this voltage-dependent temperature into Eq. (7) we can treat b as a fit parameter, which describes the magnitude of the heating. If our heating model is valid, $b\propto\sqrt{R_\square/R}$. In Fig. 10 the fitted values of b are plotted as a function of $\sqrt{R_\square/R}$ for the three samples. Within the error bars it is consistent with the proportionality to $\sqrt{R_\square/R}$ as we have proposed it with our heating model. The plotted line is a least-square fit with the assumption that for $\sqrt{R_\square/R}=0$ (i.e., ideal reservoirs) no heating is present. The values of b are higher by a factor of 1.8 than expected from our model. A higher thermal resistance between electron and phonon temperature $R_{e\text{-}ph}$ would scale with $\sqrt{R_\square/R}$ as well. Such a contribution can, however, be ruled out. Although the relevant parameter $\Gamma=5\times10^9\ \mathrm{m^{-2}\,K^{-3}}$, which was obtained in a 20-nm-thick Au film, could be smaller in the reservoir due to a larger diffusion coefficient, such an increase would be negligible. A contribution from a Kapitza resistance would be independent of $R_\square/R$. A calculation using $\sigma_K=100\ \mathrm{W/m^2\,K^4}$ would explain in maximum an increase of 22 mK corresponding to a change in b of about 23 K/V, which again is negligible.

In view of the current debate of a possibly enhanced electron-electron interaction, it is important to identify whether the additional shot noise originates from heating or from electron-electron scattering. A possible contribution to the noise arising from electron-electron scattering is, however, independent of $R_\square/R$ and would thus shift the values of b by a constant offset. From Fig. 10 we can estimate such a contribution in our data to be less than 100 K/V, corresponding to an increase of $0.01\times2e|I|$ in the asymptotic limit (see below).

The nearly linear dependence of b with $\sqrt{R_\square/R}$ proves that the major part of the additional noise in our experiment can solely be explained by thermal heating due to a temperature gradient in the reservoir and that the wires are indeed in the noninteracting regime.

Our measurements support experimental results by Schoelkopf *et al.* who compared measured differential noise on short diffusive wires with the interacting and noninteracting theories and found good agreement only for the noninteracting regime, hence the 1/3 theory. These experiments were performed at lower voltages where heating effects are less important (Fig. 6). However, the absolute slope of S_I in the asymptotic limit could not be extracted in that paper. An absolute value has been reported by Steinbach *et al.* The measured slope was, however, found to be significantly larger than 1/3. They explained the increase of noise partly by heating and partly by residual electron-electron interactions and proposed to use the shot-noise measurement for an independent measurement of the electron-electron interaction in thin metal films. The uncertainty on how large the electron-electron scattering really is, has led to the experiment by Pothier *et al.*,[18] who directly measured the electron-distribution function by tunneling spectroscopy. Based on those results we have estimated the residual contribution from electron-electron scattering in our wires. The only relevant parameter is the ratio of the dwell time of an electron in the wire $\tau_D=L^2/D=70$ ps to the scattering parameter $\tau_0=1$ ns from Ref. 18. A numerical simulation is used to calculate the electron-distribution function $f(E,x)$ in the wire. Inserting this distribution into Eq. (4), we obtain the shot noise, which is now slightly larger than $1/3\times2e|I|$ in the asymptotic limit. This increase due to electron-electron scattering is, however, only of the order of $0.007\times2e|I|$. As mentioned above our data displayed in Fig. 10 is not in contradiction, since the error bars would allow for an offset independent of $R_\square/R$ of the order of $0.01\times2e|I|$.

V. CONCLUSION

In this paper we have shown that for a metallic diffusive wire a shot-noise power consistent with the universal value $1/3\times2e|I|$ is experimentally obtained in the asymptotic limit $eV\gg kT$ if the reservoirs are designed to minimize a temperature rise as current flows through the wire. This implies that the ratio between wire resistance R and reservoir-sheet resistance $R_\square$ should be large, i.e., of the order of 1000 to avoid a large temperature gradient due to electronic heat diffusion from the wire region into the reservoirs. The lateral reservoir size is set by the electron-phonon scattering length. To avoid a difference between the electron and phonon temperatures, the radius of the reservoir should be at least $2l_{e\text{-}ph}$. In a very striking manner, our experiments demonstrate that shot-noise reduction factors close to $\sqrt{3}/4$ can be measured in the asymptotic limit even for wires that *must* be in the independent-electron regime. Though we have a hold of the universial 1/3 noise-suppression factor for diffusive wires in the noninteracting electron regime, another lesson can be drawn from the present experiments: In all highly nonequilibrium electric-transport experiments conducted at low temperatures one has to include the complete environment up to macroscopically large distances. In this respect experiments differ markedly from the approach of a theorist, who can separate the wire from the environment by imposing ideal boundary conditions. However, ideal boundaries (reservoirs) are nontrivial in real experiments.

ACKNOWLEDGMENTS

We would like to thank H. Pothier for providing us with the computer program to calculate the electron distribution function in the out-of-equilibrium regime. Fruitful discussions with M. Büttiker, D. Loss, and E.V. Sukhorukov are gratefully acknowledged. This paper was supported by a grant from the Swiss National Science Foundation.

[1] For a recent review, see M. J. M. de Jong and C. W. J. Beenakker, in *Shot Noise in Mesoscopic Systems* in *Mesoscopic Electron Transport*, Vol. 345 of *NATO Advanced Studies Institute, Series E: Applied Sciences*, edited by L. P. Kouwenhoven, G. Schön, and L. L. Sohn (Kluwer Academic, Dordrecht, 1996), and references therein.

[2] M. B. Johnson, Phys. Rev. **29**, 367 (1927); H. Nyquist, *ibid.* **32**, 110 (1928).

[3] W. Schottky, Ann. Phys. (Leipzig) **57**, 541 (1918).

[4] H. Birk, M. J. M. de Jong, and C. Schönenberger, Phys. Rev. Lett. **75**, 1610 (1995).

[5] M. Reznikov, M. Heiblum, H. Shtrikman, and D. Mahalu, Phys. Rev. Lett. **75**, 3340 (1995); A. Kumar, L. Saminadayar, D. C. Glattli, Y. Jin, and B. Etienne, *ibid.* **76**, 2778 (1996); R. C. Liu, B. Odom, Y. Yamamoto, and S. Tarucha, Nature (London) **391**, 263 (1998).

[6] A. H. Steinbach, J. M. Martinis, and M. H. Devoret, Phys. Rev. Lett. **76**, 3806 (1996).

[7] C. W. J. Beenakker and M. Büttiker, Phys. Rev. B **46**, 1889 (1992).

[8] K. E. Nagaev, Phys. Lett. A **169**, 103 (1992).

[9] A. Shimizu and M. Ueda, Phys. Rev. Lett. **69**, 1403 (1992); A. Shimizu, M. Ueda, and H. Sakaki, Proceedings of the 4th International Symposium on Foundations of Quantum Mechanics, Tokyo, 1992 [Jpn. J. App. Phys. **9**, 89, 1993].

[10] M. J. M. de Jong and C. W. J. Beenakker, Phys. Rev. B **51**, 16 867 (1995).

[11] T. González, C. González, J. Mateos, D. Pardo, L. Reggiani, O. M. Bulashenko, and J. M. Rubi, Phys. Rev. Lett. **80**, 2901 (1998).

[12] E. V. Sukhorukov and D. Loss, Phys. Rev. Lett. **80**, 4959 (1998).

[13] R. Landauer, Physica B **227**, 156 (1996).

[14] M. Büttiker (private communication).

[15] F. Liefrink and J. I. Dijkhuis, M. J. M. de Jong, L. W. Molenkamp, and H. van Houten, Phys. Rev. B **49**, 14 066 (1994).

[16] B. L. Altshuler, A. G. Aronov, and D. E. Khmelnitskii, J. Phys. C **15**, 7367 (1982).

[17] R. J. Schoelkopf, P. J. Burke, A. A. Kozhevnikov, D. E. Prober, and M. J. Rooks, Phys. Rev. Lett. **78**, 3370 (1997).

[18] H. Pothier, S. Guéron, N. O. Birge, D. Estéve, and M. H. Devoret, Phys. Rev. Lett. **79**, 3490 (1997).

[19] Sh. Kogan, *Electronic Noise and Fluctuations in Solids* (Cambridge University Press, Cambridge, England, 1996).

[20] R. Landauer, IBM J. Res. Dev. **1**, 233 (1957); D. S. Fisher and P. A. Lee, Phys. Rev. B **23**, 6851 (1981); M. Büttiker, Phys. Rev. Lett. **57**, 1761 (1986); IBM J. Res. Dev. **32**, 317 (1988).

[21] V. A. Khlus, Zh. Éksp. Teor. Fiz. **93**, 2179 (1987) [Sov. Phys. JETP **66**, 1243 (1987)]; G. B. Lesovik, Pis'ma Zh. Éksp. Teor. Fiz. **49**, 513 (1989) [JETP Lett. **49**, 592 (1989)]; M. Büttiker, Phys. Rev. Lett. **65**, 2901 (1990); Physica B **175**, 199 (1991); Phys. Rev. B **46**, 12 485 (1992).

[22] K. E. Nagaev, Phys. Rev. B **52**, 4740 (1995).

[23] M. J. M. de Jong, Ph.D. thesis, Leiden University, 1995.

[24] F. C. Wellstood, C. Urbina, and J. Clarke, Phys. Rev. B **49**, 5942 (1994).

[25] M. L. Roukes, M. R. Freeman, R. S. Germain, R. C. Richardson, and M. B. Ketchen, Phys. Rev. Lett. **55**, 422 (1985).

[26] M. Henny, H. Birk, R. Huber, C. Strunk, A. Bachtold, M. Krüger, and C. Schönenberger, Appl. Phys. Lett. **71**, 773 (1997).

[27] D. C. Glattli, P. Jacques, A. Kumar, P. Pari, and L. Saminadayar, J. Appl. Phys. **81**, 7350 (1997).